Brain Advance Access published May 19, 2006

doi:10.1093/brain/awl111 *Brain* (2006) Page 1 of 11

Unconscious vision: new insights into the neuronal correlate of blindsight using diffusion tractography

Sandra E. Leh,[1] Heidi Johansen-Berg[2] and Alain Ptito[1]

[1]Cognitive Neuroscience Unit, Montreal Neurological Institute and Hospital, McGill University, Montreal, Canada and [2]Centre for Functional Magnetic Resonance Imaging of the Brain, Department of Clinical Neurology, University of Oxford, Oxford, UK

Correspondence to: Alain Ptito and Sandra Leh, Neuropsychology/Cognitive Neuroscience Unit, Montreal Neurological Institute,
3801 University Street, Montreal, Quebec, Canada, H3A 2B4
E-mail: alain.ptito@mcgill.ca; sandra@bic.mni.mcgill.ca

The existence of several types of unconscious vision, or 'blindsight', has convincingly been demonstrated in numerous studies, and their neuronal correlates have been hypothesized according to the nature of the residual vision observed. We used diffusion tensor imaging (DTI) tractography to demonstrate an association between the presence of 'Type I'- blindsight or 'attention blindsight' and reconstructed superior colliculi (SC) fibre tracts in hemispherectomized subjects, in support of the hypothesis that this subcortical structure plays a pivotal role in this type of blindsight. Before the DTI study, 'Type I' blindsight was identified in two of four hemispherectomized subjects by using a spatial summation effect paradigm, an indirect behavioural method, in which subjects were unaware of a stimulus presented in their blind visual field and were required to respond to an identical stimulus presented simultaneously in their intact field. SC tracts were then reconstructed in six control subjects, the two hemispherectomized subjects with blindsight and the two hemispherectomized subjects without blindsight. Whereas control subjects demonstrated mainly ipsilateral connections to visual association areas, parietal cortex, prefrontal areas and to an area close to the frontal eye fields, hemispherectomized subjects with blindsight showed ipsi- and contralateral connections from the SC to visual association areas, primary visual areas, parietal areas, prefrontal areas and to the posterior part of the internal capsule. In contrast, no projections from the SC on the hemispherectomized side were observed in hemispherectomized subjects without blindsight, in support of a key role of this structure in 'Type-I' or 'attention blindsight'.

Keywords: blindsight; diffusion tensor imaging (DTI) tractography; superior colliculus; hemispherectomized subjects; brain plasticity

Abbreviations: DTI = diffusion tensor imaging; FEF = frontal eye fields; FMRIB = functional MRI of the brain; MNI = Montreal Neurological Institute; SC = superior colliculi

Received January 11, 2006. Revised March 29, 2006. Accepted March 30, 2006.

Introduction

A lateralized cortical lesion of the primary visual area has traditionally been thought to result in total blindness in the contralateral visual field. However, evidence has accumulated that residual visual functions remain after retrogeniculate lesions of the visual pathways. The ability to respond to visual stimuli in the blind visual field without acknowledged awareness has been termed 'blindsight' (Weiskrantz *et al.*, 1974).

Since the early reports of blindsight, a wide range of residual functions with and without awareness has been described. The visual abilities of subjects without acknowledged awareness have been called 'Type I' blindsight (Weiskrantz, 1989). They are far-ranging and include target detection and localization by saccadic eye movements (Pöppel *et al.*, 1973) or manual pointing (Weiskrantz *et al.*, 1974), movement direction detection, relative velocity discrimination (Barbur *et al.*, 1980; Weiskrantz *et al.*, 1995) as well as stimulus orientation detection (Weiskrantz, 1986).

Some subjects also show 'Type II' blindsight (Weiskrantz, 1989) characterized by residual visual abilities with awareness such as consciously detecting a fast-moving stimulus and its

direction (Weiskrantz *et al.*, 1995) or semantic priming from words presented in the blind field (Marcel, 1998). Because of the variety of residual behaviours demonstrated by blindsight patients, Danckert and Rossetti (2005) have recently suggested a new taxonomy: (i) 'action blindsight' is observed when an action is used to guess the localization of a target by pointing or saccading in the blind field; (ii) 'attention blindsight' is associated with motion direction detection and implicit task interference effects of a stimulus presented in the blind visual field. Here, attentional processes appear to contribute without necessarily involving a specific action. Conscious awareness of the stimulus presented in the blind visual field may or may not accompany this kind of blindsight phenomenon; (iii) 'agnosopsia' (Zeki and Ffytche, 1998) is used to describe the ability of the patient to guess the correct perceptual characteristic of the target in spite of being completely unaware of its presence in the blind field. This would include residual visual abilities that involve form or wavelength discrimination.

As suggested by us previously (for example, Bittar *et al.*, 1999), Danckert and Rossetti's classification system (2005) assumes that blindsight is mediated by subcortical neural structures that were not affected by the cortical damage and the ensuing degeneration (Boire *et al.*, 2001). They classify perceptual processing such as form and wavelength discrimination as 'agnosopsia' presumably mediated by interlaminar layers of the dLGN, and 'action blindsight' and 'attention blindsight' as implicating the retinofugal pathway from the eye to the superior colliculi (SC) but differing in the regions of extrastriate cortex involved.

Whereas ipsilesional extrastriate cortices have been proposed as responsible for blindsight in subjects with restricted posterior lesions, we have suggested subcortical structures (such as the SC) possibly in conjunction with the remaining hemisphere, as likely contenders in subjects who have had a whole cerebral hemisphere removed or disconnected from the rest of the brain. Although behavioural studies have been fairly convincing about the existence of blindsight in these subjects (Ptito *et al.*, 2001), neuroimaging research using functional MRI (fMRI) has been unable to show a connection between functional activity in the SC and blindsight probably owing to the methodological limitations of the technique (Sahraie *et al.*, 1997; Bittar *et al.*, 1999).

Advances in diffusion tensor imaging (DTI) tractography have provided new approaches for investigating cerebral connectivity because this technique enables reconstruction of white matter tracts *in vivo* (Jones *et al.*, 1999; Mori *et al.*, 1999) and tracing of pathways between grey matter structures (Behrens *et al.*, 2003*a*). With the aim of improving our understanding of the neuronal correlate of blindsight and brain plasticity and reorganization in hemispherectomized subjects with and without blindsight, we used DTI tractography to identify SC connections of these subjects.

In DTI, the magnetic resonance signal is sensitized to the random motion (diffusion) of water molecules, to provide local measures of the magnitude of water diffusion, which can be related to fibre structure in the brain (Basser *et al.*, 1994). Diffusion is anisotropic in white matter (in contrast to CSF, for example, in which diffusion is isotropic), with the preferred direction of diffusion parallel to axons. Hence, fibre tracts consisting of coherently oriented axons can be visualized using DTI, which provides us with measurements of the preferred directions of diffusion at each voxel, the degree of anisotropy of the diffusion displacement distribution and the average magnitude of diffusion. Further, computational analysis can be used to reconstruct white matter fibre tracts in 3D, allowing assessment of connectivity between different regions (Conturo *et al.*, 1999; Jones *et al.*, 1999; Mori *et al.*, 1999). In the present study, we used a probabilistic diffusion tractography algorithm (Behrens *et al.*, 2003*a*) that is able to trace likely fibre pathways between grey matter structures (Behrens *et al.*, 2003*b*).

Methods

Subjects

We recruited six healthy control subjects, who had no history of neurological or ophthalmological diseases, and four postoperative hemispherectomy patients (average intelligence) with a well-documented hemianopia without macular sparing (DR, SE, FD, JB, *see* Table 1) who had participated in previous visual research projects.

Hemispherectomy is a relatively rare surgery usually carried out for the treatment of intractable epilepsy that involves massive removal or disconnection of an entire cerebral hemisphere including the occipital lobe. These subjects are unique because any evidence of blindsight cannot be attributed to spared islands of occipital cortex (Wessinger *et al.*, 1996) and a direct geniculo-extrastriate-koniocellular projection, which has been previously suggested as an explanation for blindsight (Sincich *et al.*, 2004), does not exist.

All participating hemispherectomized subjects were previously tested for blindsight in a behavioural experiment (S.E. Leh, K.T. Mullen and A Ptito, in preparation) before this DTI study. Briefly, human vision involves three post-receptor mechanisms, an

Table 1 Hemispherectomized subjects participating in this study

Subject	Sex	Aetiology	Surgery type	Side	Blindsight
SE	Male	Right porencephalic cyst	Partial hemispherectomy	R	Yes
DR	Female	Rasmussen's encephalitis	Functional hemispherectomy	R	Yes
JB	Male	Left porencephalic cyst	Functional hemispherectomy	L	No
FD	Female	Meningitis, right middle cerebral artery infarct	Functional hemispherectomy	R	No

achromatic one consisting of retinal input from the long-wavelength-sensitive (L-) and medium-wavelength-sensitive (M) cones (L/M additive luminance system), and two colour mechanisms consisting of an antagonistic comparison of signals from the three different retinal cone types (L, M, S cones). The L/M cone opponent colour system is sensitive to red–green, and the S/(L + M) cone opponent colour system is sensitive to blue–yellow (Marrocco and Li, 1977; Schiller and Malpeli, 1977; Sumner *et al.*, 2002; Savazzi and Marzi, 2004). Since the SC is not receiving any retinal S-cone input, it is presumed that it is colour-blind to isoluminant blue/yellow stimuli (for review, *see*, for example, McKeefry *et al.*, 2003; Mullen and Kingdom, 2002). Such knowledge allowed us to make precise predictions regarding the residual visual abilities of hemispherectomized subjects. The test consisted of bilaterally and unilaterally presented achromatic black/white as well as blue/yellow gabor patches to isolate either the achromatic or the blue/yellow colour pathway using a spatial summation effect paradigm. The spatial summation effect paradigm is well known and represents a form of implicit processing or 'attention-blindsight' in that the mean reaction times to two bilaterally presented stimuli are significantly faster than to a single stimulus presented to the intact field. This implies that the simultaneous presentation of a second stimulus in the blind field can alter the mean reaction time to the consciously perceived stimulus in the intact field. While only a response to the consciously perceived stimulus is required, attention blindsight is demonstrated if the subject responds more quickly to two stimuli, one of which is in the blind field, than to a single one in the intact field. In our study, the subjects were never aware of the stimulus presentations in their blind visual field and they never responded by a key-press to single stimulus presentations made in their blind field. Eye movements were controlled by an eye tracking device and stimuli were set on a uniform background of the same mean luminance and chromaticity to control for light scatter.

The behavioural results demonstrated faster reaction times to bilaterally presented achromatic black/white, but not to blue/yellow stimuli of two of the four hemispherectomized subjects (SE and DR), indicating that 'attention blindsight' in these subjects is unlikely to be mediated by a direct contralateral retinopulvinar connection that receives input from colour-opponent ganglion cells (Felsten *et al.*, 1983; Cowey *et al.*, 1994). Rather, we hypothesize that blindsight in hemispherectomized subjects is mediated via the SC since blue/yellow stimuli are invisible to collicular cells.

On the basis of these results and those from previous studies (*see*, for example, Tomaiuolo *et al.*, 1997; Bittar *et al.*, 1999; Leh *et al.* presented at the Annual Meeting of the Cognitive Neuroscience Society, San Francisco, CA, April 2004), the four hemispherectomized subjects were classified as 'with attention blindsight' (SE and DR) and 'without attention blindsight' (JB and FD).

Hemispherectomized subjects with 'Type I' or 'attention blindsight'

DR is a 31-year-old right-handed woman. At age 5, at onset of epileptic seizures, she was diagnosed with Rasmussen's chronic encephalitis and had a contralateral (left) homonymous hemianopia as well as a progressive left hemiparesis. At age 17, she underwent a right functional hemispherectomy including the amygdala and the hippocampus. Her level of intellectual function in 1992 was estimated using the seven-subtest short form of the revised Wechsler Adult Intelligence Scale (WAIS-R). She earned a full-scale IQ score (FSIQ) rating in the average range (83), with the performance IQ (PIQ) (83) and the verbal IQ (VIQ) (87) in the same range (for further details, *see*, for example, Bittar *et al.*, 1999).

SE is a 40-year-old right-handed man. A left hemiparesis was noted at birth, and seizure onset was at age 7. At age 25, the hemispherectomy (temporo-parieto-occipital removal) was performed to alleviate intractable seizures due to a congenital porencephalic cyst (for further details, *see*, for example, Wessinger *et al.*, 1996). His intellectual level was estimated in 1991 using the seven-subtest short form of the WAIS-R. He earned a FSIQ rating in the average range (93), with the PIQ (99) and the VIQ (90) in the same classification.

Hemispherectomized subjects without 'Type I' or 'attention blindsight'

FD is a 23-year-old right-handed woman. Her seizures started at age 1. In 2000, at age 18, she underwent a right hemispherectomy and became seizure-free after surgery. Her intellectual level was estimated in 2005 using the seven-subtest short form of the WAIS-R. Although she showed below-average performances in most domains tested, it was felt that the results obtained underestimated her everyday life skills and that her cognitive abilities would improve steadily as she had become seizure-free and interference with cerebral function was now minimal.

JB is a 40-year-old left-handed man. He had a congenital right hemiparesis with seizure onset at age 5. A left functional hemispherectomy was performed in two steps (1983 and 1985), in order to remove a congenital porencephalic cyst. The frontal and occipital poles were left in place to prevent superficial haemosiderosis and reduce hydrocephalus but were disconnected from the rest of the brain (for further details, *see*, for example, Wessinger *et al.* 1996). JB's intellectual functions are in the low average range (FSIQ 88), with the PIQ (88) and the VIQ (90) in the same classification.

Data acquisition

T_1-weighted anatomical MRI images and diffusion-weighted images were obtained at the Brain Imaging Centre of the Montreal Neurological Institute (MNI) on a 1.5 T Siemens Sonata scanner using echoplanar imaging (EPI) with a standard head coil. The following parameters were used for diffusion-weighted data: repetition time: 9300 ms, echo time: 94 ms, flip angle: 90°, slice thickness = 2.2 mm, number of slices: 60, in-plane resolution: 2.1875 mm × 2.1875 mm, acquisition time: ~9 min and 30 s. Diffusion weighting was performed along 60 independent directions, with a *b*-value of 1000 s/mm^2. A reference image with no diffusion weighting was also obtained.

Image preprocessing

Diffusion-weighted raw data were processed using the tools of the FMRIB Software Library [FSL, version 5.0; Oxford Centre for Functional MRI of the Brain (FMRIB), UK; www.fmrib.ox.ac.uk/fsl; for detailed description of methods, *see* Behrens *et al.*, 2003*a*; Smith *et al.*, 2004]. We first corrected for eddy current distortions and motion artefacts using the eddy current correction tool within the FMRIB's Diffusion Toolbox (FDT, version 1.0). Following eddy current and motion correction, we extracted the skull from the T_1-images using the Brain Extraction Tool. We then fitted diffusion tensors at each voxel independently to the data and co-registered diffusion-weighted images to the anatomical image using a six-parameter transform of the FMRIB Linear Image Registration

Tool. Diffusion modelling and probabilistic tractography were carried out using the FDT (version 1.0), which allows for an estimation of the most probable location of a pathway from a seed point using Bayesian techniques (Oxford Centre for Functional MRI of the Brain, FSL, version 5.00, UK; www.fmrib.ox.ac.uk/fsl). Fibre tracking was initiated from all voxels within the seed masks to generate 5000 streamline samples, with a step length of 0.5 mm and a curvature threshold of 0.2. Anatomical images were transformed to standard space using the MNI coordinates with a 12-point transformation (MNI 152 brain, Evans *et al.*, 2003). Raw tracts of healthy subjects were thresholded at least at 20 samples (out of the 5000 generated from each seed voxel), binarized and summed across subject to obtain a population map, which was then thresholded to display only those voxels that were present in at least 33% of subjects. The probabilistic tractography approach uses sampling techniques to draw samples through the probability estimate on fibre direction at each voxel. We generate 5000 of these samples from each voxel. In resulting connectivity distributions, voxel values represent the number of these samples passing through any given voxel. The lower the number of samples, the lower the probability of a pathway through the voxel. We chose to use a threshold of 20 samples to remove only those voxels with very low connectivity probability. Figure 1 and Table 2 show the effect of thresholding tracts at 2, 20 and 200 samples for a normal subject, a subject without blindsight and a subject with blindsight. Note that the results of reconstructed tracts are robust independently of the threshold being used. We are therefore confident that we were able to rule out potential threshold effects.

Study 1

Corticospinal tract seed mask

The hemispherectomized subjects showed contralateral upper limb paresis but no hemiplegia and normal ipsilateral motor function. In study 1, we chose the intact corticospinal tract in hemispherectomy subjects as a control tract to validate our DTI data quality and analysis methods as we expected it to be similar to that of normal subjects. To do this, we defined seed masks on the fractional anisotropy (FA) maps of each subject within the corticospinal white matter of the cerebral peduncle. Fibre tracking was initiated from all voxels within the seed masks. Seed masks were defined on the FA maps of each subject including 20 voxels within the corticospinal white matter of the cerebral peduncle.

Results

Corticospinal tracts

Reconstructed right and left corticospinal tracts that were present in at least 33% of the healthy subjects are presented in Fig. 2A. Reconstructed tracts of the remaining hemisphere in hemispherectomized subjects without blindsight are demonstrated in Fig. 2B and in subjects with blindsight in Fig. 2C. Note that the intact corticospinal tracts of all hemispherectomized subjects are very similar to the reconstructed

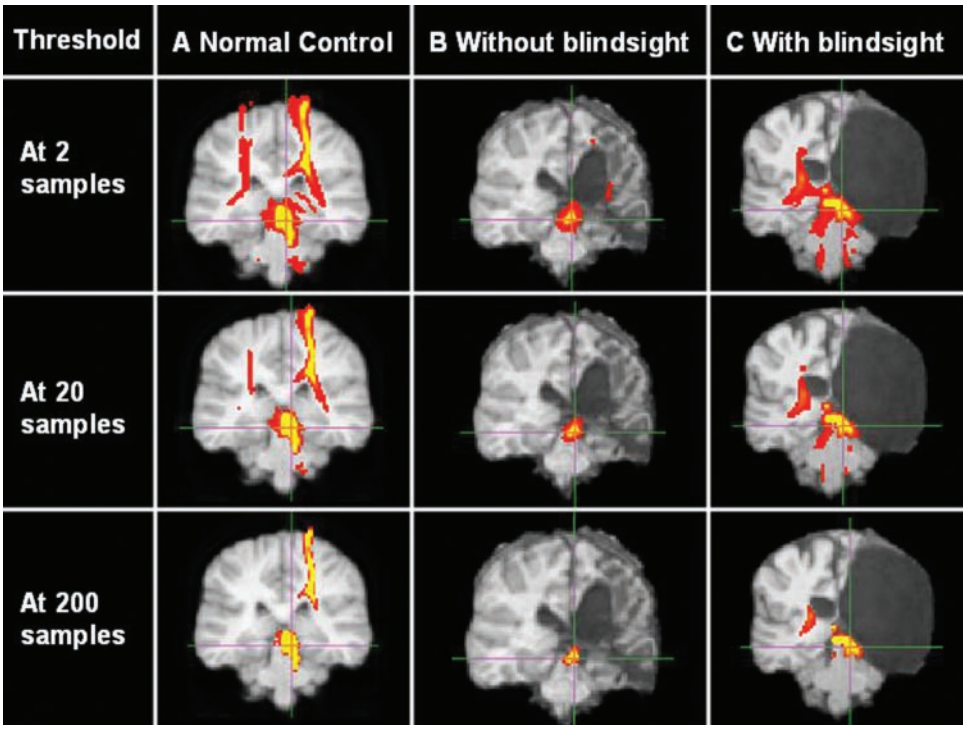

Fig. 1 Robustness of the effect of threshold on samples passing through a voxel in control and hemispherectomized subjects. The figure shows the effect of thresholding tracts at 2, 20 and 200 on samples for a normal control subject (**A**), a subject without blindsight (**B**) and a subject with blindsight (**C**) (slice level at right superior colliculus: $x = 8$, $y = -34$, $z = 12$). In hemispherectomized subjects SC tracts from the hemispherectomized side to the contralateral remaining hemisphere are shown. Note the robustness of reconstructed tracts independently of the threshold being used.

Table 2 Robustness of sample threshold and presence of fibre connections in hemispherectomized subjects

	FEF	Visual association areas	Parietal-occipital areas	Prefrontal areas	Primary visual areas	Internal capsule
(A) Hs with blindsight (SE)						
Sample threshold for ipsilateral projections						
2	+	+	+	+	+	–
20	+	+	+	+	+	–
200	+	+	+	+	–	–
(B) Hs with blindsight (DR)						
Sample threshold for contralateral projections						
2	+	–	–	–	–	+
20	+	–	–	–	–	+
200	+	–	–	–	–	+
(C) Hs without blindsight (FD)						
Sample threshold for projections from the hemispherectomized side						
2	–	–	–	–	–	–
20	–	–	–	–	–	–
200	–	–	–	–	–	–
(D) Hs without blindsight (JB)						
Sample threshold for projections from the hemispherectomized side						
2	–	–	–	–	–	–
20	–	–	–	–	–	–
200	–	–	–	–	–	–

Table showing the presence of a specific connection and the robustness of these numbers to sample threshold used. Results are shown for hemispherectomized subjects (Hs) with (A, B) and without blindsight (C, D) for the connections from the superior colliculus of the hemispherectomized side to the contralateral hemisphere.

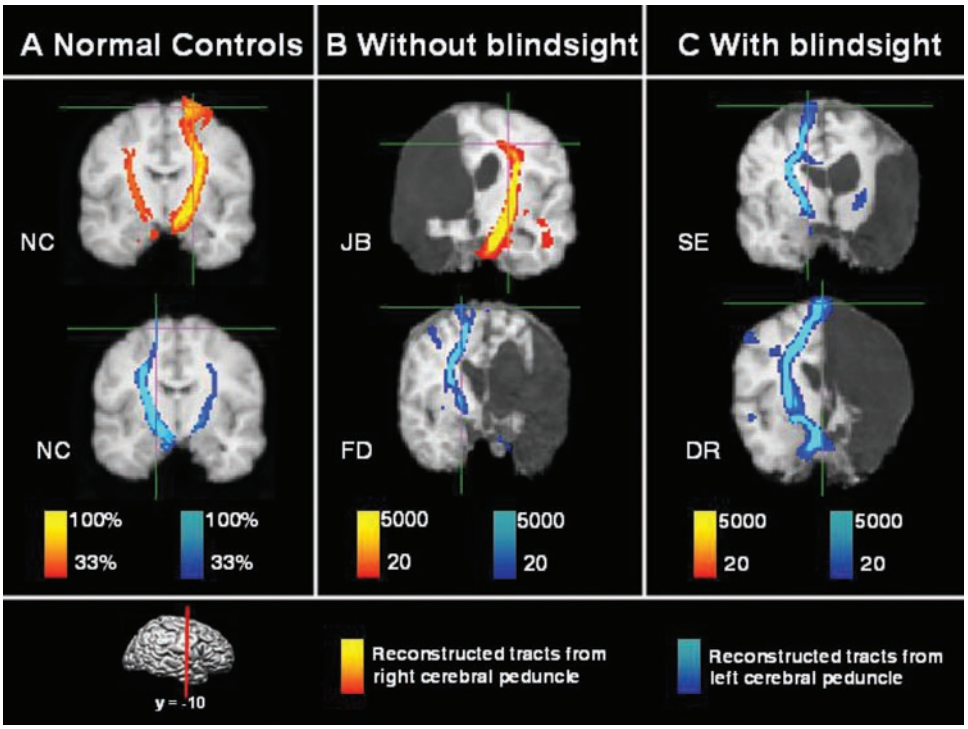

Fig. 2 Illustration of reconstructed corticospinal tracts. Images are displayed in MNI standard stereotaxic space. (**A**) Thresholded map of the right (red hues) and the left (blue hues) reconstructed corticospinal tract present in at least 33% of the healthy subjects. (**B**) Reconstructed corticospinal tracts in two hemispherectomized subjects without blindsight (JB, FD). (**C**) Reconstructed corticospinal tracts in two hemispherectomized subjects with blindsight (SE, DR). The saturation of the colour (intensity of colour scale) in **B** and **C** indicates the voxel value in the connectivity distribution, which represents the number of samples that passed through that voxel: the lighter the colour of the tract (yellow or light blue), the higher the probability of a connection passing through this voxel. Note that reconstructed corticospinal tracts are very similar in healthy and hemispherectomized subjects.

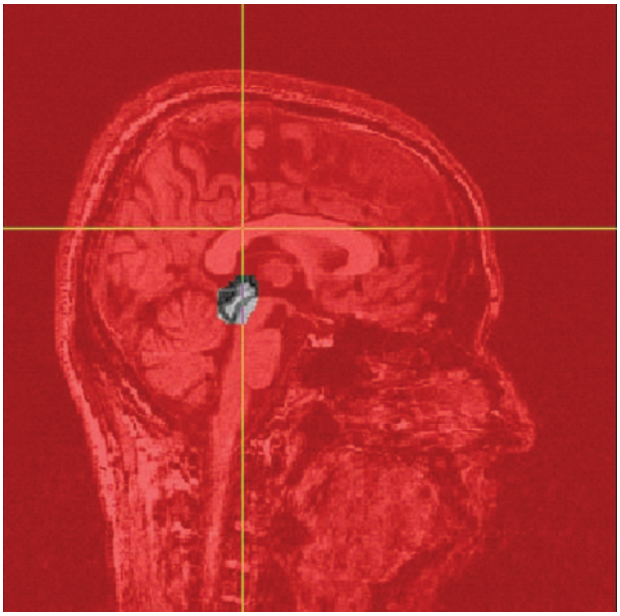

Fig. 3 Exclusion mask.

corticospinal tracts in healthy subjects, and are in accordance with the known anatomy of this tract, demonstrating that accurate fibre tracking is possible in all datasets.

Study 2

Reconstruction of superior colliculi tracts

Superior colliculi seed mask

First, we created seed masks on each subject's T_1-weighted image, including the whole SC. To exclude the possibility that the absence of contralateral pathways in hemispherectomized subjects without blindsight could be due to the smaller size of their seed masks due to collicular degeneration, we ran a further analysis in which seed masks of a fixed size of 24 voxels were placed in the centre of the SC in all subjects. The results obtained with the fixed size masks were very similar to those obtained with the original masks—healthy controls and hemispherectomized subjects with blindsight showing contralateral paths from SC, in contrast to the hemispherectomized subjects without blindsight who did not.

Exclusion mask

We created a single sagittal slice along the midline on the T_1-image of each subject leaving a gap only around the SC (Fig. 3). This allowed us to restrict analyses only to those paths that cross at the level of the SC.

Results

Superior colliculi tracts

A seed mask of the right and left SC was created on each subject's T_1-weighted anatomical image (*see* Methods). Tracts from all voxels in the SC to the rest of the brain were then reconstructed in the same fashion as described above for the corticospinal tracts. For interhemispheric connections, we restricted our analysis to include only those tracts that cross the midline at the level of the SC (*see* Methods). After reconstructing fibre tracts of the left and right SC in healthy subjects, we registered the images to MNI standard stereotaxic space and created a thresholded map across subjects (Fig. 4). Note the similarity of individual tracts in healthy subjects in Fig. 5.

Healthy subjects showed ipsilateral connections to visual association areas (Fig. 4C; $x = \pm 28$, $y = -74$, $z = 20$) and to the parietal-occipital cortex (Fig. 4B; $x = \pm 32$, $y = -50$, $z = 50$). Additional ipsilateral projections were found close to an area (right SC: $x = 18$, $y = -6$, $z = 50$; left SC: $x = -20$, $y = -6$, $z = 46$) that has previously been described as frontal eye fields (FEF; Paus, 1996; $x = \pm 24$ to ± 40, $y = -6$ to 1, $z = 44$ to 51; Fig. 4A) and to prefrontal areas (Fig. 4D; $x = \pm 20$, $y = 62$, $z = 2$), but not to primary visual areas (Fig. 4E; $x = \pm 2$, $y = -90$, $z = 0$). These results are consistent with anatomical studies showing direct retinal input to the SC and bidirectional connections between the SC and occipital areas (for example, Rushmore and Payne, 2003), as well as bidirectional connections between the SC and the FEF (for example, Stanton *et al.*, 1988; Lynch *et al.*, 1994; Gaymard *et al.*, 2003). Ipsi- and contralateral connections in healthy subjects also projected to the internal capsule posterior to the corticospinal tract. At that level, the limitations of DTI technology did not permit differentiation between visual and motor pathways, although these findings are consistent with the known projections from the SC to frontal and parietal cortical areas via the posterior part of the internal capsule and their presumed role in triggering inhibitory saccades (*see*, for example, Gaymard *et al.*, 2003; Condy *et al.*, 2004).

Results of the two hemispherectomized subjects without 'Type I' or 'attention blindsight' are displayed in Fig. 6 (JB) and in Fig. 7 (FD). Both subjects showed an absence of connections to other cortical areas observed in healthy subjects (Figs 6 and 7, from the hemispherectomized side to the contralateral remaining hemisphere). The ipsilateral projections that were seen were weaker than those in healthy subjects, and were only observed from the ipsilateral SC to the cuneus (Figs 6C and 7E, from the healthy side to the ipsilateral remaining hemisphere). We interpret this lack of projections as an indication of considerable degeneration of both SC in the two subjects without 'Type I' or 'attention blindsight'.

In contrast, the two hemispherectomized subjects with 'Type I' or 'attention blindsight' (DR and SE; Figs 8 and 9) showed strong contralateral and ipsilateral projections from the SC to the remaining hemisphere. Strong ipsilateral and contralateral projections to an area close to the FEF (Fig. 8A; $x = 18$, $y = -2$, $z = 50$), to parieto-occipital areas (Fig. 8B; $x = -20$, $y = -56$, $z = 48$), to visual association areas (Fig. 8C; $x = -28$, $y = -74$, $z = 20$; $x = -4$, $y = -90$, $z = -22$) and to primary visual areas (Fig. 8E; $x = -2$, $y = -90$,

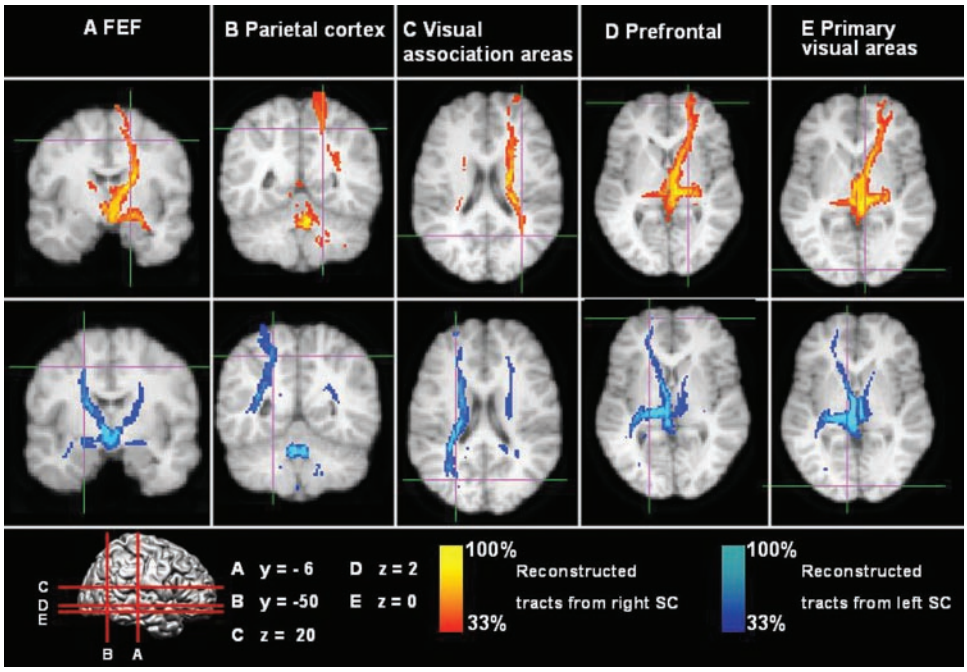

Fig. 4 Population probability maps of reconstructed SC tracts based on tractography in six healthy subjects. Fibre tracking was initiated from a seed mask in the right superior colliculus demonstrated in red hues and from a seed mask in the left superior colliculus demonstrated in blue hues. Intensity of the colour scales represents the proportion of the population showing a tract at any given voxel. Tracts were registered to MNI standard stereotaxic space, thresholded at 20 samples, binarized and summed across subjects. For individual subject tracts, see Fig. 5. Images demonstrate ipsilateral projections close to an area (right superior colliculus: $x = 18$, $y = -6$, $z = 50$; left superior colliculus: $x = -20$, $y = -6$, $z = 46$) that has previously been described as FEF (**A**; Paus, 1996: $x = \pm 24$ to ± 40, $y = -6$ to 1, $z = 44$ to 51), to the parietal-occipital cortex (**B**; $x = \pm 32$, $y = -50$, $z = 50$), visual association areas (**C**; $x = \pm 28$, $y = -74$, $z = 20$) and the prefrontal areas (**D**; $x = \pm 20$, $y = 62$, $z = 2$), but not to primary visual areas (**E**; $x = \pm 2$, $y = -50$, $z = 0$).

$z = 0$) were notable in subject SE. SE also showed ipsi- and contralateral projections to spared prefrontal areas on the hemispherectomized side (Fig. 8D; $x = 12$, $y = 64$, $z = 2$). In DR, reconstructed tracts indicate ipsi- and contralateral projections to the posterior internal capsule (Fig. 9F; $x = -20$, $y = -20$, $z = 12$) and to areas close to the FEF (Fig. 9A; $x = -20$, $y = -10$, $z = 44$), an area known to be involved in visual tasks such as saccade generation and orientation (for example, Stanton *et al.*, 1988; Lynch *et al.*, 1994).

Discussion

Our results indicate the presence of projections from the contralateral and ipsilateral SC to the remaining hemisphere in hemispherectomized subjects with 'Type I' or 'attention blindsight' and an absence of those projections in the subjects without 'Type I' or 'attention blindsight', thereby confirming our assumption (Tomaiuolo *et al.*, 1997; Bittar, *et al.*, 1999) and that of Danckert and Rossetti (2005) that blindsight is mediated by a collicular route. Interestingly, the contralateral connections in subjects with 'Type I' or 'attention blindsight', which crossed at the level of the SC, were more prominent than the crossed projections seen in healthy controls.

Previous anatomical studies on the connectivity of the SC have demonstrated an excitatory and an inhibitory intercollicular circuitry (Olivier *et al.*, 2000; Rushmore *et al.*, 2003) as well as restoration of visual orientation in hemianopic cats by modulating SC function (for example, Ciaramitaro *et al.*, 1997; Sherman, 1977). The SC is the main recipient of retinal projections in lower mammals with a phylogenetically older and more primitive visual system than humans. Similar but weaker retinocollicular projections also exist in humans, however, and were demonstrated in a recent single case study in which visual orientation was restored in a left-sided neglect patient after an additional lesion of the contralateral SC (Weddell, 2004). Although existing SC connections to the remaining cortical areas seem to play a pivotal role in unconscious vision, blindsight subjects remain unaware of the information processed in their blind visual field. One possibility for the lack of awareness may lie in the lack of synchronicity in cerebral activation. The human visual pathways process information simultaneously and yet are able to work independently of each other (as is the case following a circumscribed lesion in a visual cortical area) (Rees *et al.*, 2002; Naghavi and Nyberg, 2005). For conscious perception, however, a specific synchronized activation pattern of different cortical areas involving ventral, parietal and frontal visual areas is believed to be crucial (for further details, *see*, for example, Beck *et al.*, 2001; Rees *et al.*, 2002; Naghavi and Nyberg, 2005). Our results indicate that hemispherectomized subjects with 'Type I' or

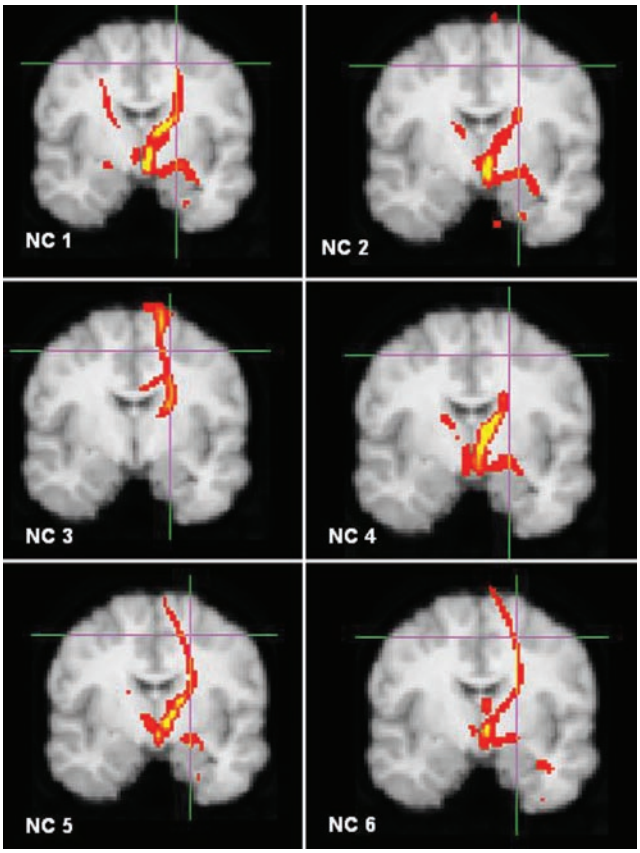

Fig. 5 Examples of individual SC tracts in six control subjects (NC 1–6). Tracts (slice level for right superior colliculus: $x = 22$, $y = -6$, $z = 50$) have been thresholded at 20 samples, and intensity of colour scale indicates the number of samples that passed through that voxel from red (low probability of connection) to yellow (high probability of connection).

'attention blindsight' are able to enhance visual performance in their blind field, but remain unaware of visual processing presumably because they are unable to access a more complex synchronous cortical activation pattern involving higher top-down mechanisms necessary for conscious vision.

Limitations of DTI

Diffusion tractography is a relatively new technique and there are a number of methodological limitations that should be taken into account in the interpretation of the results. First, it is not possible to differentiate between anterograde and retrograde connections using DTI such that we cannot establish whether estimated pathways are travelling to or from the SC. Previous tracer studies on non-human primates, however, suggest that there are bidirectional connections between the SC and the FEF (*see*, for example, Stanton *et al.*, 1988; Lynch *et al.*, 1994; Gaymard *et al.*, 2003), occipital areas (*see*, for example, Rushmore and Payne, 2003) and to the posterior part of the internal capsule (*see*, for example, Gaymard *et al.*, 2003; Condy *et al.*, 2004). This is likely to be the case in humans.

A second limitation of our approach concerns the interpretation of the presence or absence of a particular pathway in the diffusion data. There is good evidence that in coherent white matter regions the direction of maximum diffusion corresponds with the principal fibre direction (Lin *et al.*, 2001), and that tractography in such regions corresponds well with human post-mortem data (Stieltjes *et al.*, 2001). In regions of fibre complexity, of crossing, or of degeneration, however, the relationship between the paths that can be traced through the diffusion data and the underlying fibre architecture is not as clear and is still not fully understood.

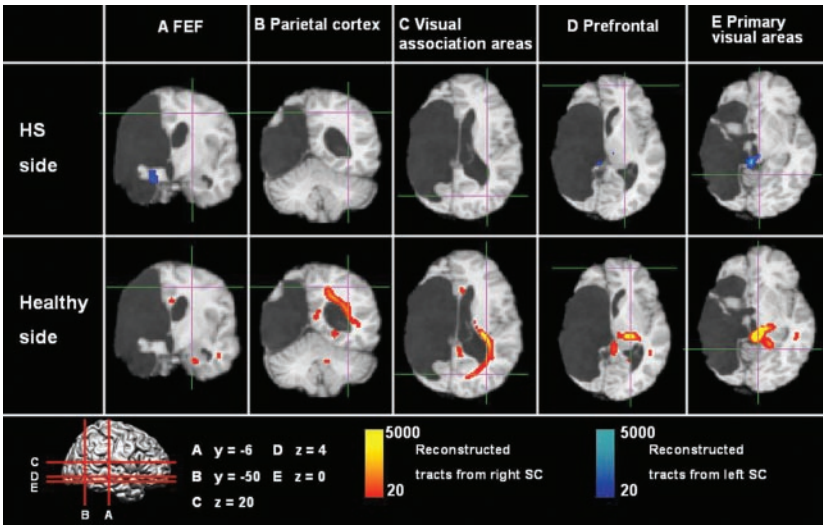

Fig. 6 Illustration of reconstructed right (red hues) and left (blue hues) SC tracts in a hemispherectomized subject without Type I blindsight (without attention blindsight) (JB). The saturation of the colour (intensity of the colour scale) indicates the voxel value in the connectivity distribution, which represents the number of samples that passed through the voxel: the lighter the colour of the tract (yellow or light blue), the higher the number of probable fibres passing through this voxel. Reconstructed SC tracts of JB demonstrate almost no contralateral connections, and projections between the ipsilateral SC and other cortical areas suggest degeneration of both SC.

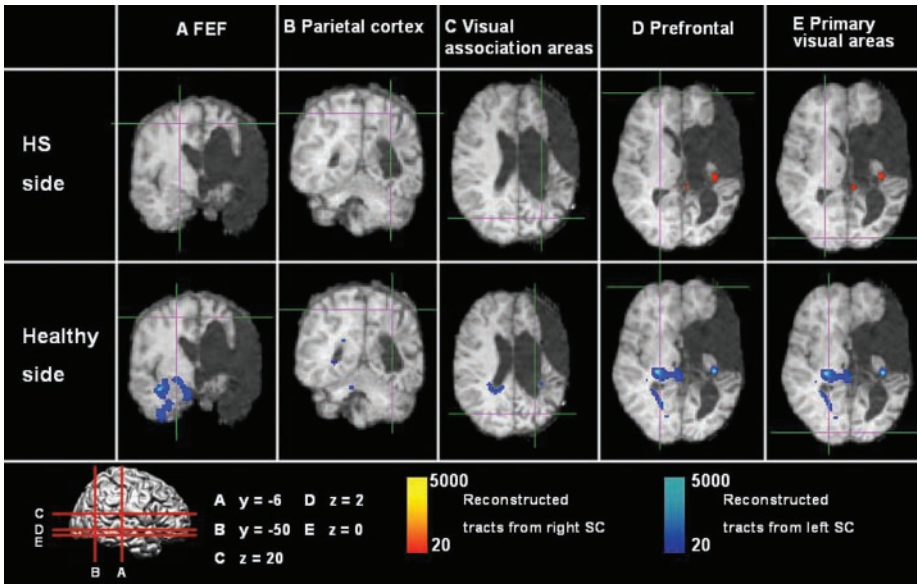

Fig. 7 Illustration of reconstructed right (red hues) and left (blue hues) SC tracts in a hemispherectomized subject without Type I blindsight (without attention blindsight) (FD). The saturation of the colour (intensity of the colour scale) indicates the voxel value in the connectivity distribution, which represents the number of samples that passed through the voxel: the lighter the colour of the tract (yellow or light blue), the higher the number of probable fibres passing through this voxel. Reconstructed SC tracts of FD demonstrate almost no contralateral connections, and projections between the ipsilateral SC and other cortical areas suggest degeneration of both SC.

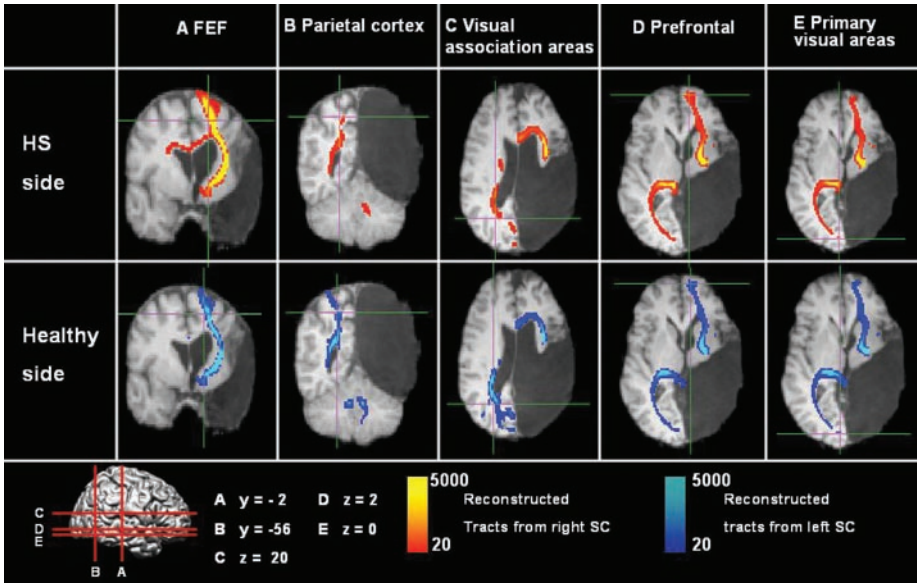

Fig. 8 Illustration of reconstructed right (red hues) and left (blue hues) SC tracts in a hemispherectomized subject with Type I blindsight (attention blindsight) (SE). The saturation of the colour (intensity of the colour scale) indicates the voxel value in the connectivity distribution, which represents the number of samples that passed through the voxel: the lighter the colour of the tract (yellow or light blue), the higher the probability of a pathway passing through this voxel. SE showed strong contra- and ipsilateral connections to an area close to the FEF (**A**; $x = 18$, $y = -2$, $z = 50$), to parieto-occipital areas (**B**; $x = -20$, $y = -56$, $z = 48$), to visual association areas (**C**; $x = -4$, $y = -90$, $z = -22$) and to primary visual areas (**E**; $x = -2$, $y = -90$, $z = 0$). SE also showed ipsi- and contralateral projections to spared prefrontal areas on the hemispherectomized side (**D**; $x = 12$, $y = 64$, $z = 2$).

The absence of a particular pathway through the diffusion data in one group of subjects is consistent with the lack of an underlying anatomical route in that group, but cannot prove that no anatomical route exists. Other factors, such as data quality, FA, or path geometry may also influence the ability to trace pathways through the diffusion data. By demonstrating that all participating subjects in the present study, including the subjects without blindsight, showed similar tracings

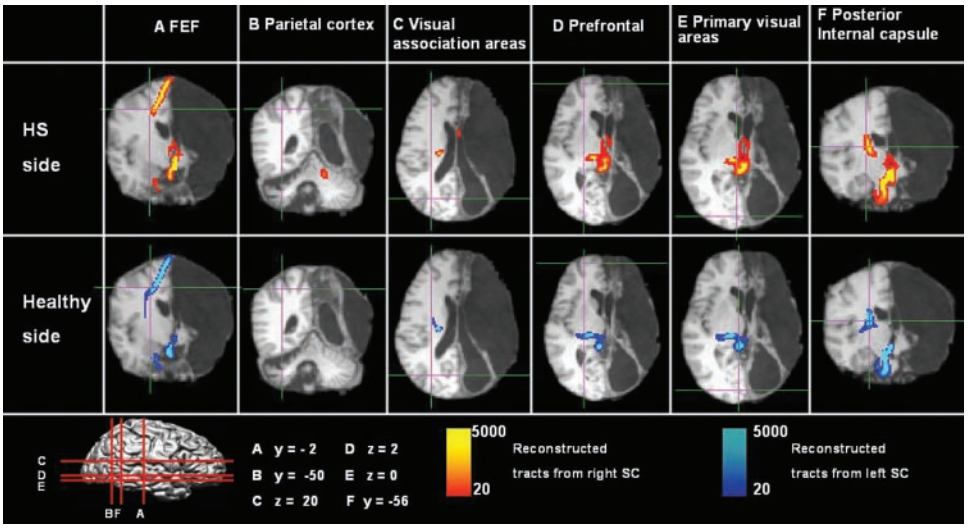

Fig. 9 Illustration of reconstructed right (red hues) and left (blue hues) SC tracts in a hemispherectomized subject with Type I blindsight (attention blindsight) (DR). Reconstructed tracts of DR indicate ipsi- and contralateral projections to the posterior internal capsule (**F**; $x = 20$, $y = -20$, $z = -16$) and to areas close to the FEF (**A**; $x = -20$, $y = -10$, $z = 44$).

of the corticospinal tracts, we believe we have provided an argument against a general effect on data quality in our patients without blindsight. It remains possible, however, that differences in diffusion tractography performance reflect localized differences in tract integrity, rather than a complete absence of a crossed anatomical route from the SC to the remaining hemisphere in patients without blindsight.

Conclusion

We were able to demonstrate the existence of strong ipsilateral and contralateral projections from the SC to primary visual areas, visual association areas, precentral areas/FEF and the internal capsule of the remaining hemisphere only in those hemispherectomized subjects with 'Type I' or 'attention blindsight'. No such connections could be identified in those hemispherectomized subjects without 'Type I' or 'attention blindsight'. These results strongly support an essential role of the SC in blindsight. This study also demonstrates the usefulness of DTI tractography in investigating cerebral plasticity, compensation and reorganization following various cerebral lesions.

Acknowledgements

We would like to thank the subjects for their time and participation. We thank David Flitney, Sylvain Milot and Jean-Francois Malouin for their technical support. We are grateful to Alan Evans, Michael Petrides, Bruce Pike, John Robson, Jonathan Seal, Jürgen Germann, Timothy Behrens and Natalie Voets for their input and discussions on previous versions of the manuscript. This study was supported by a REPRIC training award to S.E.L. on DTI analysis techniques (University of Oxford, UK), a doctoral scholarship from CRIR to S.E.L. and an NSERC research grant to A.P. (RGPIN 37354-02).

Competing Interests Statement: The authors declare that they have no competing financial interests.

References

Barbur JL, Ruddock KH, Waterfield VA. Human visual responses in the absence of the geniculo-calcarine projection. Brain 1980; 103: 905–28.

Basser PJ, Mattiello J, LeBihan D. Estimation of the effective self-diffusion tensor from the NMR spin echo. J Magn Reson B 1994; 103: 247–54.

Beck DM, Rees G, Frith CD, Lavie N. Neural correlates of change detection and change blindness. Nat Neurosci 2001; 4: 645–50.

Behrens TE, Woolrich MW, Jenkinson M, Johansen-Berg H, Nunes RG, Clare S, et al. Characterization and propagation of uncertainty in diffusion-weighted MR imaging. Magn Reson Med 2003a; 50: 1077–88.

Behrens TE, , Johansen-Berg H, Woolrich MW, Smith SM, Wheeler-Kingshott CA, Boulby PA, et al. Non-invasive mapping of connections between human thalamus and cortex using diffusion imaging. Nat Neurosci 2003b; 6: 750–7.

Bittar RG, Ptito M, Faubert JS, Dumoulin O, Ptito A. Activation of the remaining hemisphere following stimulation of the blind hemifield in hemispherectomized subjects. Neuroimage 1999; 10: 339–46.

Boire D, Theoret H, Ptito M. Visual pathways following cerebral hemispherectomy. Prog Brain Res 2001; 134: 379–97.

Ciaramitaro WE, Todd WE, Rosenquist AC. Disinhibition of the superior colliculus restores orienting to visual stimuli in the hemianopic field of the cat. J Comp Neurol 1997; 387: 568–87.

Condy C, Rivaud-Pechoux S, Ostendorf F, Ploner CJ, Gaymard B. Neural substrate of antisaccades: role of subcortical structures. Neurology 2004; 63: 1571–8.

Conturo TE, Lori NF, Cull TS, Akbudak E, Snyder AZ, Shimony JS, et al. Tracking neuronal fiber pathways in the living human brain. Proc Natl Acad Sci USA 1999; 96: 10422–7.

Cowey A, Stoerig B, Bannister M. Retinal ganglion cells labelled from the pulvinar nucleus in macaque monkeys. Neuroscience 1994; 61: 691–705.

Danckert J, Rossetti Y. Blindsight in action: what can the different sub-types of blindsight tell us about the control of visually guided actions? Neurosci Biobehav Rev 2005; 29: 1035–46.

Evans AC, Collins DL, Mills SR, Brown ED, Kelly RL. 3-D statistical neuroanatomical models from 305 MRI volumes. In: Proceedings IEEE-Nuclear Science Symposium and Medical Imaging Conference, 2003; 1813–7.

Felsten G, Benevento LA, Burman D. Opponent-color responses in macaque extrageniculate visual pathways: the lateral pulvinar. Brain Res 1983; 288: 363–7.

Gaymard B, Lynch J, Ploner CJ, Condy C, Rivaud-Pechoux S. The parieto-collicular pathway: anatomical location and contribution to saccade generation. Eur J Neurosci 2003; 17: 1518–26.

Jones DK, Simmons A, Williams SC, Horsfield MA. Non-invasive assessment of axonal fiber connectivity in the human brain via diffusion tensor MRI. Magn Reson Med 1999; 42: 37–41.

Leh SE, Armony J, Ptito A. Blindsight and the processing of complex stimuli: a behavioural study of a hemispherectomized patient. Cognitive Neuroscience Society, Annual Meeting, San Francisco, CA, April 2004.

Lin CP, Tseng WY, Cheng HC, Chen JH. Validation of diffusion tensor magnetic resonance axonal fiber imaging with registered manganese-enhanced optic tracts. Neuroimage 2001; 14: 1035–47.

Lynch JC, Hoover JE, Strick PL. Input to the primate frontal eye field from the substantia nigra, superior colliculus, and dentate nucleus demonstrated by transneuronal transport. Exp Brain Res 1994; 100: 181–6.

Marcel AJ. Blindsight and shape perception: deficit of visual consciousness or of visual function? Brain 1998; 121: 1565–88.

Mori S, Crain BJ, Chacko VP, van Zijl PC. Three-dimensional tracking of axonal projections in the brain by magnetic resonance imaging. Ann Neurol 1999; 45: 265–9.

Naghavi HR, Nyberg L. Common fronto-parietal activity in attention, memory, and consciousness: shared demands on integration? Conscious Cogn 2005; 14: 390–425.

Marrocco RT, Li RH. Monkey superior colliculus: properties of single cells and their afferent inputs. J Neurophysiol 1977; 40: 844–60.

McKeefry DJ, Parry NR, Murray IJ. Simple reaction times in color space: the influence of chromaticity, contrast, and cone opponency. Invest Ophthalmol Vis Sci 2003; 44: 2267–76.

Mullen KT, Kingdom FA. Differential distributions of red-green and blue-yellow cone opponency across the visual field. Vis Neurosci 2002; 19: 109–18.

Olivier E, Corvisier J, Pauluis Q, Hardy O. Evidence for glutamatergic tectotectal neurons in the cat superior colliculus: a comparison with GABAergic tectotectal neurons. Eur J Neurosci 2000; 12: 2354–66.

Paus T. Location and function of the human frontal eye-field: a selective review. Neuropsychologia 1996; 34: 475–83.

Pöppel E, Held R, Frost D. Residual visual function after brain wounds involving the central visual pathways in man. Nature 1973; 243: 295–6.

Ptito A, Fortin A, Ptito M. 'Seeing' in the blind hemifield following hemispherectomy. Prog Brain Res 2001; 134: 367–78.

Rees G, Kreiman G, Koch C. Neural correlates of consciousness in humans. Nat Rev Neurosci 2002; 3: 261–70.

Rushmore RJ, Payne BR. Bilateral impact of unilateral visual cortex lesions on the superior colliculus. Exp Brain Res 2003; 151: 542–7.

Sahraie A, Weiskrantz L, Barbur JL, Simmons A, Williams SCR, Brammer MJ. Pattern of neuronal activity associated with conscious and unconscious processing of visual signals. Proc Natl Acad Sci USA 1997; 94: 9406–11.

Savazzi S, Marzi CA. The superior colliculus subserves interhemispheric neural summation in both normals and patients with a total section or agenesis of the corpus callosum. Neuropsychologia 2004; 42: 1608–18.

Schiller PH, Malpeli JG. Properties and tectal projections of monkey retinal ganglion cells. J Neurophysiol 1977; 40: 428–45.

Sherman SM. The effect of superior colliculus lesions upon the visual fields of cats with cortical ablations. J Comp Neurol 1977; 172: 211–30.

Sincich LC, Park KF, Wohlgemuth MJ, Horton JC. Bypassing V1: a direct geniculate input to area MT. Nat Neurosci 2004; 7: 1123–8.

Smith SM, Jenkinson M, Woolrich MW, Beckmann CF, Behrens TE, Johansen-Berg H, et al. Neural correlates of consciousness in humans. Neuroimage 2004; 23 Suppl 1: S208–19.

Stanton GB, Goldberg ME, Bruce CJ. Frontal eye field efferents in the macaque monkey. II. Topography of terminal fields in midbrain and pons. J Comp Neurol 1988; 271: 493–506.

Stieltjes B, Kaufmann WE, van Zijl PC, Fredericksen K, Pearlson GD, Solaiyappan M, et al. Diffusion tensor imaging and axonal tracking in the human brainstem. Neuroimage 2001; 14: 723–35.

Sumner P, Adamjee T, Mollon JD. Signals invisible to the collicular, magnocellular pathways can capture visual attention. Curr Biol 2002; 12: 1312–6.

Tomaiuolo F, Ptito M, Marzi CA, Paus T, Ptito A. Blindsight in hemispherectomized patients as revealed by spatial summation across the vertical meridian. Brain 1997; 120: 795–803.

Weddell RA. Subcortical modulation of spatial attention including evidence that the Sprague effect extends to man. Brain Cogn 2004; 55: 497–506.

Weiskrantz L. Blindsight: a case study and implications. Oxford: Clarendon Press; 1986.

Weiskrantz L. Consciousness and commentaries. In: Hameroff S, Kaszniak A, Scott A, editors. Towards a science of consciousness II—the second Tucson discussion and debates. Cambridge: MIT Press. 1989: p. 371–7.

Weiskrantz L, Warrington EK, Sanders MD, Marshall J. Visual capacity in the hemianopic field following a restricted occipital ablation. Brain 1974; 97: 709–28.

Weiskrantz L, Barbur JL, Sahraie A. Parameters affecting conscious versus unconscious visual discrimination with damage to the visual cortex (V1). Proc Natl Acad Sci USA 1995; 92: 6122–6.

Wessinger CM, Fendrich R, Ptito A, Villemure JG, Gazzaniga MS. Residual vision with awareness in the field contralateral to a partial or complete functional hemispherectomy. Neuropsychologia 1996; 34: 1129–37.

Zeki S, Ffytche DH. The Riddoch syndrome: insights into the neurobiology of conscious vision. Brain 1998; 121: 25–45.